Macrocyclic peptides targeting human CD44 inhibit cell adhesion

Chatzopoulos, A.; Kolliopoulos, C.; Yin, Y.Z.; Karalis, T.; Komine, A.; Tran, S.T.P.; ... ; Heldin, P.

Cellular Signalling 136 (2025) 112178

Contents lists available at ScienceDirect

Cellular Signalling

journal homepage: www.elsevier.com/locate/cellsig

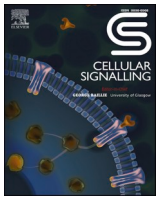

Macrocyclic peptides targeting human CD44 inhibit cell adhesion

Athanasios Chatzopoulos [a,b,1], Constantinos Kolliopoulos [a,1], Yizhen Yin [c,d,1], Theodoros Karalis [a], Aya Komine [e], Sophie T. PhuongDung Tran [f,k], Jongchan Hwang [f,g,k], Nohara Goto [f,h,k], Hiroaki Suga [c], Peter ten Dijke [i,j], Christopher John Hipolito [i,*], Spyridon S. Skandalis [b,*], Paraskevi Heldin [a,*]

[a] Department of Medical Biochemistry and Microbiology, Uppsala University, SE-751 23 Uppsala, Sweden
[b] Biochemistry, Biochemical Analysis & Matrix Pathobiology Res. Group, Laboratory of Biochemistry, Department of Chemistry, University of Patras, 26504 Patras, Greece
[c] Department of Chemistry, Graduate School of Science, The University of Tokyo, 7-3-1 Hongo, Bunkyo-ku, Tokyo 113-0033, Japan
[d] State Key Laboratory of Microbial Technology, Shandong University, Qingdao 266237, China
[e] Department of Experimental Pathology, Graduate School of Comprehensive Human Sciences and Faculty of Medicine, University of Tsukuba, Ibaraki, Japan
[f] Human Biology, School of Integrative and Global Majors, University of Tsukuba, 1-1-1 Tennodai, Tsukuba 305-8575, Japan
[g] Department of Oncology, St. Jude Children's Research Hospital, 262 Danny Thomas Place, Memphis, TN 38105-3678, USA
[h] Asahi Kasei Pharma, Izunokuni-shi, Shizuoka, Japan
[i] Department of Cancer Signaling, Graduate School of Comprehensive Human Sciences and Faculty of Medicine, University of Tsukuba, Tsukuba, Ibaraki, Japan
[j] Oncode Institute and Department of Cell and Chemical Biology, Leiden University Medical Center, Leiden, the Netherlands
[k] Department of Experimental Pathology, Faculty of Medicine, University of Tsukuba, Japan

ARTICLE INFO

Keywords:
Hyaluronan
CD44
Cancer cells
Macrocyclic peptides

ABSTRACT

CD44-hyaluronan interactions play a significant role in the progression of aggressive tumors. We generated non-native ligands for CD44 by identifying macrocyclic peptides that interact with the hyaluronan-binding domain of CD44. We investigated how the macrocyclic peptides L4–3 and D4–3 influence hyaluronan-engaged CD44 signaling in tumor cells, with a focus on glioma cells, as well as normal fibroblasts.

Our findings indicated that inhibiting hyaluronan binding to CD44 in cultured U251MG glioma cells using the macrocyclic peptides L4–3 or D4–3 led to a reduction in cell adhesion and impacted various signaling pathways. The activation of hyaluronan-engaged CD44 during glioma progression - an aggressive and heterogeneous disease associated with multiple oncogenic alterations – cross-talk with epidermal growth factor receptor (EGFR) signaling. Specifically, the macrocyclic peptide L4–3 enhanced the negative feedback regulation of EGFR autophosphorylation at Tyr1068, an effect induced by phorbol 12-myristate 13-acetate (PMA). Furthermore, L4–3 inhibited EGF-mediated activation of the serine/threonine kinase AKT in glioma cells. These findings illuminate the relationship between the CD44-hyaluronan axis and EGFR signaling, suggesting a possible therapeutic strategy.

Additionally, the macrocyclic peptide D4–3 suppressed hyaluronan-CD44-mediated adhesion and affected signaling related to cellular adhesion and migration in fibroblasts. However, it did not influence AKT and ERK1/2 signaling pathways. Thus, it is possible that the inhibitory effect of macrocyclic peptides L4–3 and D4–3 on hyaluronan-CD44 interaction have different effects in different cell types.

1. Introduction

Hyaluronan, an abundant glycosaminoglycan in the extracellular matrix (ECM), plays important roles in the organization of tissue architecture, as well as in the proper development and function of the ECM. An aberrant accumulation of hyaluronan has been detected in pathological conditions, such as cancer and inflammation, where a plethora of growth factors and cytokines are released; furthermore, tumor-promoting agents, such as phorbol 12-myristate 13-acetate (PMA), promote hyaluronan synthase 2 (HAS2)-production of

* Corresponding authors.
E-mail addresses: chris.john.hipolito@gmail.com (C.J. Hipolito), skandalis@upatras.gr (S.S. Skandalis), evi.heldin@imbim.uu.se (P. Heldin).
[1] These authors equally contributed to this article.

https://doi.org/10.1016/j.cellsig.2025.112178
Received 18 May 2025; Received in revised form 10 September 2025; Accepted 15 October 2025
Available online 22 October 2025

hyaluronan, which correlates with poor outcome of tumor patients [1–4]. Hyaluronan's cellular functions primarily depend on its interaction with the plasma membrane glycoprotein CD44. This protein is encoded by a single gene that consists of 21 exons and plays a crucial role in maintaining homeostasis and is involved in various disease processes [5–7]. The CD44 gene encodes the standard form, CD44s, along with several variant isoforms (CD44v1-v11), that are formed through alternative splicing [8]. The variant CD44 isoforms are incorporated into a specific site within the membrane-proximal section of the CD44 ectodomain [9,10]. The hyaluronan-binding domain is located in the ectodomain of all CD44 isoforms, which also interacts with growth factors and their receptors, promoting intracellular signaling. CD44 can undergo two sequential proteolytic cleavages in response to immunological and oncogenic signals. The first cleavage of CD44 leads to the release of its soluble ectodomain, which plays a crucial role in the dynamic regulation of the interaction between CD44-expressing cells and the extracellular matrix during cell migration [11]. This event also results in the formation of a CD44 transmembrane-intracellular domain (CD44 TM-ICD). This process subsequently initiates the intramembranous cleavage of CD44 by presenilin (PS)-dependent γ-secretase [11–13], releasing CD44 ICD, which then translocates to the nucleus.

Once in the nucleus, the ICD forms complexes with various transcription factors that regulate, not only the expression of the CD44 gene, but also the expression of cell cycle regulators and c-MYC [14–18]. The downstream signaling pathways triggered by CD44 ICD are highly complex, and the underlying molecular mechanisms are still being investigated. While several studies have suggested that CD44 expression may serve a prognostic role in cancer progression, the correlation between CD44 expression and prognosis varies and depends on the tumor type [5,15,19].

Malignant gliomas are the most aggressive brain tumor. Most patients with this disease die in less than a year, despite multimodality therapy. The treatments include surgical resection, radiation therapy and chemotherapy, but have limited therapeutic efficacy. This can be explained by the heterogeneity of the disease, its ability to resist chemotherapy, and its invasiveness [20–22]. Glioma cells interact with microenvironmental components, including hyaluronan, and it has been reported that CD44-hyaluronan interactions impact the disease progression, however, the underlying mechanisms have been difficult to elucidate [5,23]. About 50 % of high-grade glioblastomas show amplification of the epidermal growth factor receptor (EGFR), express the mutant EGFRvIII or contain single nucleotide mutations [24]. After ligand binding, EGFR activates several signaling pathways, including ERK-MAP-kinase (MAPK), phosphatidyl-inositol-3`-kinase (PI3K)-AKT, and members of the protein kinase C (PKC) family [25]. Activation of PKCs controls several cellular functions, in a cell type- and context-dependent manner [26]. PMA, exerts its tumor promoting activity by activating PKC, which is expressed at high levels in gliomas and other malignancies.

Macrocyclic peptides targeting specific proteins constitute an emerging class of pharmacological agents [27–29]. Due to their intermediate size (about 2000 Da), macrocyclic peptides combine beneficial properties of both traditional small molecule drugs and monoclonal antibodies. Initially, such macrocyclic peptides were isolated from living organisms, but more recently, artificially generated macrocyclic peptide libraries have been used to select for ligands against biologically relevant proteins [28,30]. In order to affect CD44-hyaluronan signaling in oncogenesis and inflammation, we have attempted to produce agonistic or antagonistic macrocyclic peptides. Here, we report the discovery of *in vitro* selected macrocyclic peptide ligands that inhibit the adhesion potential of cancer and non-cancer cells on a hyaluronan substrate and have differential effects on downstream signaling.

2. Materials and methods

2.1. Cell culture and reagents

Breast cancer Hs578T cells, human embryonic kidney cells (HEK293T) and human lung adenocarcinoma A549 cells were obtained from ATCC, glioblastoma U251MG cells were a kind gift of Dr. Bengt Westermark (Uppsala University) [31], and primary human foreskin fibroblasts AG1523, which were used up to passage 20, were purchased from Coriell Institute for Medical Research. Hs578T, A549, HEK293T and AG1523 cells were routinely cultured in complete medium Dulbecco's Modified Eagle Medium (DMEM; Sigma-Aldrich Sweden AB, Stockholm, Sweden), whereas glioblastoma U251MG cells were routinely cultured in complete RPMI-1640 medium (Sigma-Aldrich Sweden AB, Stockholm, Sweden). Media were supplemented with 10 % fetal bovine serum (FBS; Biowest, Biotech-IgG AB, Lund, Sweden), penicillin (100 Units/ml), streptomycin (100 μg/ml), and 5 mM L-glutamine (Sigma-Aldrich Sweden AB, Stockholm, Sweden). Cells were maintained at 37 °C, in 95 % humidified air and 5 % CO_2. Medium was refreshed every two days. When cultures reached approximately 80 % confluency, cells were trypsinized for 1–2 min with trypsin-EDTA (#992830/100, Statens Veterinärmedicinska Anstalt; SVA) and seeded in new cell culture dishes. Depending on the experiment, the assays were carried out in starvation medium containing 0.1 % FBS or in the presence of 10 % FBS (complete medium). 4-methylumbelliferone sodium salt (4-MU, #M1508) and PMA were purchased from MERCK (Darmstadt, Germany). Hyaluronan of high molecular mass (about 1000 kDa) was kindly provided by Dr. Ove Wik (Q-Med, Uppsala, Sweden) and hyaluronan ≤200 kDa was purchased from Hylumed Medical (Genzyme, MA, USA). EGF and PDGF-BB were purchased from PeproTech EC Ltd. Nordic (Stockholm, Sweden) or Biosource Inc. (Dacula, GA, USA). All other chemicals used in the present study were of the best commercially available grade.

2.2. In vitro selection for anti-CD44 macrocyclic peptides

The *in vitro* selection and chemical synthesis of the anti-CD44 macrocyclic peptides were performed as previously described (Fig. S1) [29,32]. In brief, two macrocyclic peptide libraries were employed. One peptide library employed ClAc-L-Tyr as an initiator and the other library employed ClAc-D-Tyr as an initiator. The elongation region for both libraries was composed of 7–15 NNK codons followed by a codon for Cys.

The dissociation constants (K_D) for the interaction between the macrocyclic peptides and CD44 ectodomain were determined by surface plasmon resonance (SPR) analysis using Biacore T200 (GE Healthcare), as described [29]. Furthermore, derivatives of some of the macrocyclic peptide ligands were synthesized by modifying the *C*-terminal ends of the macrocyclic peptides with fluorescein or biotin, as described [29].

2.3. Immunostaining and transient transfections

The construct pCAGIP(BMX)-CD44s-His10, used for the ectopic expression of CD44 in HEK293T cells, was essentially constructed as previously described [33,34]. Briefly, the process involved the following steps: 1) The *CD44s* gene was PCR amplified from purified mRNA transcripts (ISOGENII [NIPPON GENE]) from MDA-MB-157 using the primers hCD44–5 (5'-CCGAATTCAGATCTACCATGGACAAGTTTTGG TG-3′) and hCD44–3 (5'-CCGCGGCCGCCCACCCCAATCTTCATGTCCA-3′). 2) The amplified gene was cloned into the pcDNA3-His10 vector using the *Eco*RI and *Not*I restriction sites. 3) The CD44-His10 sequence was excised from the resulting pcDNA3-CD44-His10 plasmid along with the nucleic acid sequence coding for the His10 tag using the *Bgl*III and *Xho*I restriction sites. 4) Finally, the excised fragment was cloned into a pCAGIP(BMX) vector (kindly gifted by Professor Hitoshi Niwa, RIKEN) using the BglIII and XhoI restriction sites, resulting in the construct pCAGIP(BMX)-CD44s-His10; we have modified the restriction enzyme

sites of pCAGIP vector by inserting a DNA insert containing restriction sites BglII, *Mlu*I, and XhoI in between the *Eco*RI sites of the pCAGIP. Thermocycling was performed using the GeneAmp PCR System 9700 (Applied Biosystems), and PCR products were purified using the NucleoSpin Gel and PCR Clean-up kit (TaKaRa).

HEK293T cells were transfected with 1 μg of the plasmid pCAGIP-CD44s-His10 using Lipofectamine 2000 (Invitrogen, Waltham, MA, USA), following the manufacturer's instructions. Staining was performed on non-permeabilized cultures. The cells were incubated on ice with 1 μM biotin-or fluorescein-labeled macrocyclic peptides for 30 min at 4 °C. After incubating overnight with CD44 antibodies (1 mM; provided by Professor Yukinari Kato) [35], the slides were washed twice. Next, secondary antibodies, specifically Alexa Fluor 488 goat anti-mouse (1:1000 dilution, Molecular Probes, Invitrogen, Eugene, OR, USA), were applied for four hours. Following this incubation, the slides were washed again, and TO-PRO or DAPI nuclear staining was performed, followed by washes with PBS. Finally, the slides were mounted, and images were captured using a TCS SP8 confocal laser scanning microscope (Leica Microsystems, Wetzlar, Germany). Staining using biotin-labeled macrocyclic peptides was carried out as above with the following exceptions: 1) incubation with the biotinylated peptides was performed for 1 h at 4 °C and 2) after washing away unbound peptide three times for 5 min using PBS, the cells were stained using 1:200 diluted Streptavidin-Fluorescein Isothiocyanate (FITC) Conjugate (Thermo Fisher) followed by washing with two times for 5 min using PBS.

2.4. Adhesion assay

Hyaluronan (about 1000 kDa; 0.2 mg/ml) in a solution containing *N*-hydroxysulfosuccinimide (0.184 mg/ml) (Thermo Fischer scientific, Gothenburg, Sweden) was mixed with an equal volume of 1-ethyl-3-(3′-dimethylaminopropyl) carbodiimide-HCl (0.123 mg/ml; Sigma-Aldrich Sweden AB, Stockholm, Sweden); 100 μl of the solution was then added to each well of a 96-well Covalink-NH microtiter plate (NUNC, Thermo Fischer Scientific, Gothenburg, Sweden). Separate 96-well plates were coated with Collagen type I (PureCol, Advanced BioMatrix Inc., Carlsbad, CA, USA) at a concentration of 40 μg/ml. Then, plates coupled with hyaluronan or collagen were incubated overnight at 4 °C followed by washing with PBS and blocking with 3 % bovine serum albumin (BSA) in PBS for 1 h at room temperature.

Cells were cultured in 100 mm dishes for 24 h in complete media, followed by starvation overnight. Next, the cells were treated with bovine testicular hyaluronidase PH-20 (1 U/ml) (Sigma-Aldrich Sweden AB, Stockholm, Sweden) for one hour at 37 °C to remove endogenous cell surface hyaluronan. After treatment, the cells were washed with PBS to remove the hyaluronidase and were detached using 10 mM EDTA in PBS. The cells were then centrifuged and resuspended in 0.1 % FBS in the appropriate medium. After counting, the cells were incubated in the presence or absence of macrocyclic peptides at final concentrations of 1000 nM for 30 min with end-to-end shaking at room temperature. About 100 000 cells were seeded per coated well in media containing 0.1 % BSA. Following a 45 min incubation at 37 °C, each well was washed thrice with PBS to remove any non-adherent cells. Thereafter, cells were fixed and stained with 0.5 % crystal violet in 20 % methanol for 20 min at room temperature, by shaking in the dark, then washed thoroughly to remove excess dye and dried completely. Bound dye was extracted by adding 100 % methanol and incubation for 20 min at room temperature with shaking in the dark. Absorbance was measured at 570 nm using an EnSpire Multimode Plate Reader.

2.5. In vitro wound healing assay

U251MG, AG1523, Hs578T, and A549 cells were seeded in 6-well plates at approximately 90 % confluence and incubated for 24 h in complete media, and then starved overnight. The next day, the cells were cultured in fresh complete media or starvation media, with or without 50 μg/ml hyaluronan, and with any of the macrocyclic peptides L4–3, D4–1 or D4–3, at a concentration of 1 μM, with or without 1 mM of 4-MU. To create a wound, a vertical incision, and three parallel incisions were made using a 20 μl pipette tip. The wounds were monitored at specified time intervals, using Phase-contrast microscopy (Axiovert 40 CFL, Zeiss mounted with AxioCam MRC, Carl Zeiss) and the ImageJ software program was used to quantify wound closure.

2.6. Immunoblot analysis

Glioma cells were cultured in complete media at approximately 70 % confluency in 6-well plates and starved for 24 h before undergoing treatment. They were either treated for 30 min with the macrocyclic peptide L4–3 or left untreated. Following this, the cultures were incubated for an additional 30 min with 80 nM PMA, 25 ng/ml EGF, or 50 μg/ml hyaluronan ($\leq$ 200 kDa). Similarly, fibroblast cultures were preincubated with 1 μM D4–3 before being stimulated, either with 20 μg/ml hyaluronan (1000 kDa) for 40 min or 20 ng/ml platelet-derived growth factor (PDGF-BB) for 10 min. After these treatments, the cultures were washed once with ice-cold PBS and lysed using RIPA lysis buffer (50 mM Tris-HCl (pH 8.0), 150 mM NaCl, 1 % NP-40, 0.5 % sodium deoxycholate, and 0.1 % SDS), supplemented with HALT protease and a phosphatase inhibitor cocktail (Thermo Fisher Scientific, Gothenburg, Sweden). The samples were then centrifuged for 15 min at 4 °C at 13000 rpm, and the supernatants were collected in new tubes. Then, 6× SDS-sample buffer containing 0.5 M Tris-HCl pH 6.8, 30 % glycerol, 0.6 M dithiothreitol (DTT), 10 % SDS, 0.012 % bromophenol blue was added, and the lysates were vortexed and heated for 5 min at 95 °C. Next, the protein concentration was measured by Bicinchoninic acid (BCA) assay (Thermo Fischer Scientific, Gothenburg, Sweden). Equal amounts of sample protein were subjected to SDS–polyacrylamide gel electrophoresis (SDS-PAGE) and transferred to nitrocellulose membrane (Amersham, GE Healthcare, Uppsala, Sweden), followed by blocking in 5 % BSA or non-fat dry milk in Tris buffered saline (TBS), supplemented with 0.1 % Tween 20 (TBS-T) at room temperature for 1 h. Membranes were then incubated at 4 °C overnight with primary antibodies (Table S1) that were diluted in a solution of 1 % BSA, TBS-T, supplemented with 0.02 % NaN_3. Then, membranes were washed three times with TBS-T for 5 min and incubated with goat anti-rabbit HRP or goat anti-mouse HRP secondary antibodies, diluted in 1 % BSA, TBS-T or 1 % non-fat dry milk, TBS-T at room temperature for 1 h, washed three times with TBS-T for 5 min and the proteins were detected by chemiluminescence (Millipore, MA, United States). Quantification of band intensity was performed by using the ImageJ software. Antibodies that were used for detection are summarized in Table S1.

2.7. Streptavidin pulldown of biotinylated macrocyclic peptide

Biotin-conjugated macrocyclic peptide L4–3 was added to U251MG cell cultures at various concentrations. The cultures were incubated for 30 min, followed by washing of the cells with ice-cold PBS. The cells were then lysed using a buffer containing 50 mM Tris-HCl, pH 7.4, 1 % NP-40, 100 mM NaCl, and 2 mM $MgCl_2$, supplemented with HALT protease and a phosphatase inhibitor cocktail. Next, the samples were centrifuged for 10 min at 4 °C at 13000 rpm. Then, supernatants were incubated overnight at 4 °C with or without Streptavidin-conjugated magnetic beads (#88816, Thermo Fisher Scientific), while being agitated end over end. Finally, the beads were washed five times with 50 mM Tris-HCl, pH 7.4, 1 % NP-40, 100 mM NaCl, 2 mM $MgCl_2$, after which 2× Laemmli SDS sample buffer was added. Equal protein amounts were subjected to SDS-PAGE and proteins were transferred to a nitrocellulose membrane. The binding of CD44 to biotinylated peptide was determined by incubating the membrane with anti-CD44 rabbit antibody, followed by incubation with goat anti-rabbit HRP secondary antibody, diluted in TBS, supplemented with 1 % BSA, 0.1 % Tween and

0.02 % NaN_3. CD44 protein was determined by chemiluminescence.

2.8. Cell proliferation

A short-term cell proliferation assay was conducted as previously described [36]. Briefly, 30 000 Hs578T, U251MG, and A549 cells were cultured in 96-well plates and incubated for 24 h. The medium was then replaced with medium containing 0.1 % FBS, and incubation was continued for 16 to 18 h. The cells were then incubated for 24 h with the macrocyclic peptides, diluted in medium with 0.1 % FBS. Thereafter, the cells were washed twice with PBS and stained with 100 µl of a 0.5 % crystal violet solution diluted in 20 % methanol, for 20 min at room temperature in the dark under shaking. The crystal violet dye was then washed away using distilled water. Cells were left to dry at room temperature, in the dark. Then, 100 µl of 100 % methanol was added to each well and the cell-bound dye was extracted by incubation for 20 min at room temperature, in the dark under shaking. Finally, the optical density of extracts from each well was measured at 570 nm, using an EnSpire Multimode Plate Reader.

In a long-term proliferation assay, U251MG cells were seeded in 6-well plates (100000 cells per well), in medium containing 3 % FBS. Every three days, cells were detached, counted, and re-seeded in 60-mm plates until day 6, when the number of cells was determined.

2.9. Statistical analysis

Reported values are expressed as mean ± SEM and are based on at least three independent experiments. Statistical significance was calculated by two-paired Student's *t*-test. One significance level is indicated, *i.e.*, $*p < 0.05$.

3. Results

3.1. Characterization of selected macrocyclic peptides

The *in vitro* selection of macrocyclic peptide ligands, targeting the human CD44 ectodomain, led to the identification of 11 peptides of interest (Table 1). The macrocyclic peptides were chemically synthesized and their binding affinities against CD44 were assessed *in vitro* by surface plasmon resistance (SPR; Fig. S2). L4–3 and D4–3 exhibited the highest binding affinity against CD44 with K_D values of 19.9 nM and 22.4 nM, respectively (Table 1). The sequences of the peptide hits are depicted in Fig. S3a. Next, we investigated whether the CD44 macrocyclic peptides specifically bound to the extracellular domain of CD44 on the cell surface. To visualize this interaction, we generated biotin- and fluorescein-labeled macrocyclic peptides (Fig. S3b). D4–3 exhibited a low dissociation constant (K_D), similar to L4–3, however, the fluorescein-labeled D4–3 bound far less strongly to the CD44 ectodomain than the fluorescein-labeled L4–3 (Fig. S4); possibly the fluorescein interfered with D4–3's interaction with CD44 due to steric hindrance or changes in conformation. Therefore, staining efforts focused on the use of the biotinylated peptide derivatives. Both L4–3-biotin and D4–3-biotin demonstrated strong binding affinity for CD44 compared to an unrelated negative control peptide, R4–1-biotin, as determined by confocal fluorescence microscopy (Fig. 1).

Table 1
Determination of affinity of generated macrocyclic peptides against hCD44-Fc by Surface Plasmon Resonance (SPR) technique.

Macrocyclic peptides	k_a ($10^4 \cdot M^{-1} \cdot s^{-1}$)	k_d ($10^{-3} \cdot s^{-1}$)	K_D (nM)
L4–1	23.5	22.3	95.1
L4–2	0.908	0.478	52.6
L4–3	**1.3**	**0.259**	**19.9**
L4–4	1.61	3.7	231
L4–6	1.15	2.83	247
D4–1	4.82	7.45	155
D4–2	0.534	0.87	163
D4–3	**3.15**	**0.704**	**22.4**
D4–4	4.08	1.26	30.8 (not reliable)
D4–5	1.84	0.594	32.3
D4–6	1.23	1.31	107

3.2. L4-3 and D4-3 regulate the adhesion, but not the motility, of glioma, lung, and breast cancer cells

We investigated the ability of CD44, expressed in glioblastoma (U251MG) (Fig. 2a), lung adenocarcinoma (A549), and invasive breast ductal carcinoma (Hs578T) (Fig. S5) cells, to adhere to plates coated with hyaluronan, in the absence and presence of macrocyclic peptides. In our previous research, we demonstrated that these cell lines predominantly express the standard form of CD44 [37–39]. The effects of macrocyclic peptides on cell adhesion to collagen-coated plates were also evaluated. The cell adhesion receptors expressed by U251MG cells, such as CD44 and integrins, showed strong adhesion to both hyaluronan- and collagen-coated plates compared to uncoated plates (Fig. 2a). Notably, L4–3 and D4–3, which bind with high-affinity to CD44, caused a significant decrease in cellular adhesion to hyaluronan-coated plates, but did not affect adhesion to collagen-coated plates. This suggests that L4–3 and D4–3 selectively bind to the extracellular domain of CD44

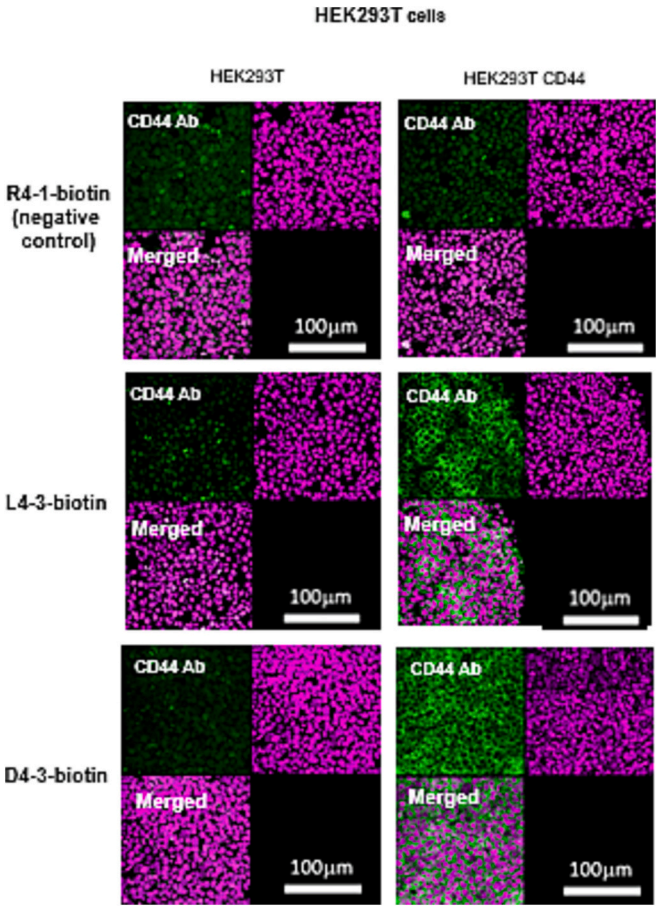

Fig. 1. Biotin-labeled macrocyclic peptides L4–3 and D4–3 bind to HEK293T cells overexpressing CD44. Wild-type HEK293T and cells ectopically expressing the standard form of CD44 (HEK293T CD44) were analyzed for the binding of the biotin-labeled L4–3 and D4–3 peptides (L4–3-biotin and D4–3-biotin), as well as the binding of a negative control peptide (R4–1-biotin), using confocal fluorescence microscopy (Nikon Eclipse 90i). Nuclei are shown in blue (TO-PRO nuclear staining,1:1000, 5 min). Scale bars 100 µm. (For interpretation of the references to colour in this figure legend, the reader is referred to the web version of this article.)

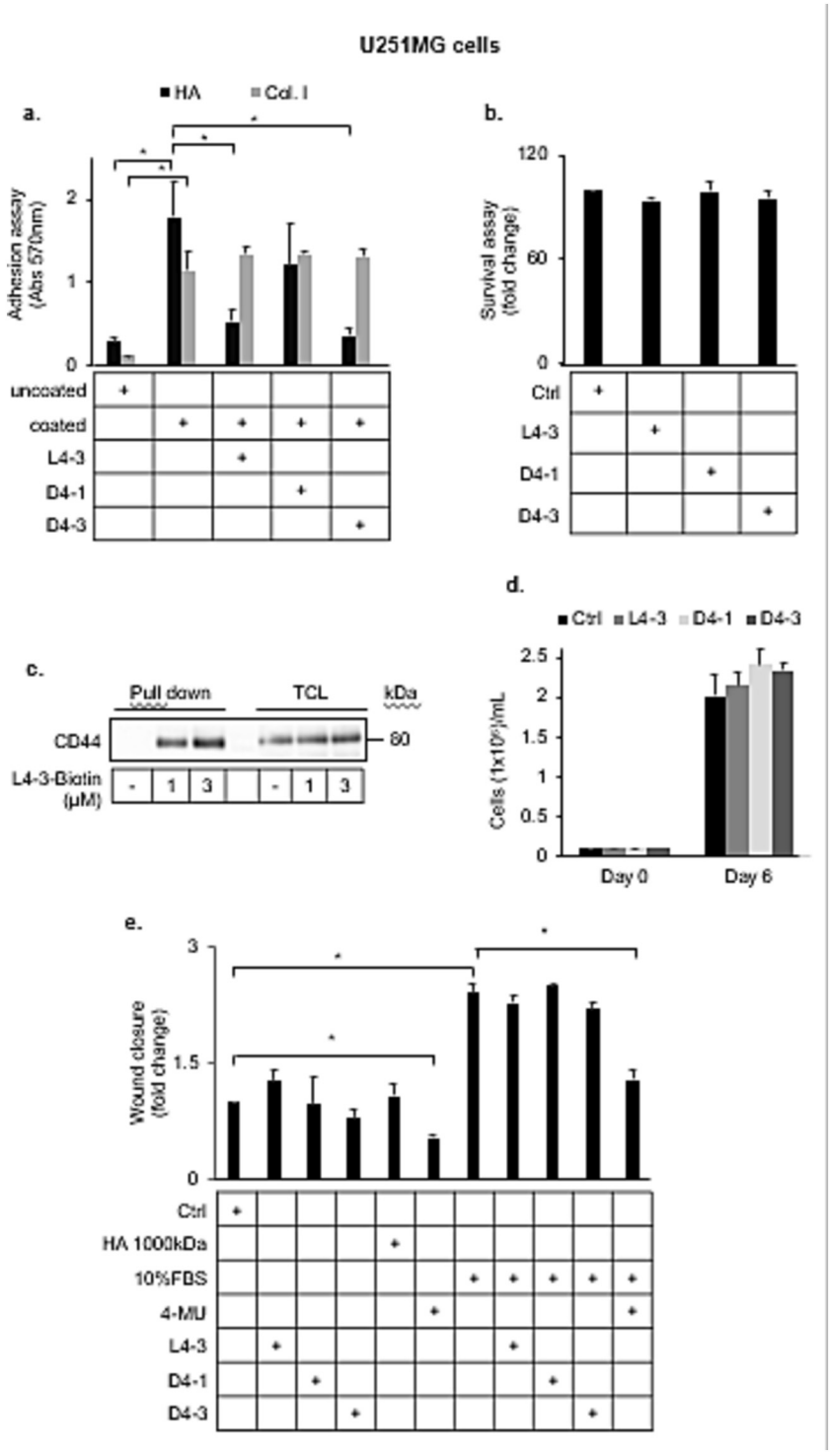

Fig. 2. Macrocyclic peptides interact with the hyaluronan receptor CD44 in glioma cells, influencing cellular adhesion, but not motility. (a) U251MG cells were starved overnight and subjected to adhesion assays on hyaluronan- and collagen type I-coated substrates, in the absence and presence of 1 μM peptides, as outlined in the Materials and Methods section. Uncoated wells served as controls. (b) A 24-h cell survival assay was conducted on U251MG cells after treatment with 1 μM of the peptides L4–3, D4–1, or D4–3 in 0.1 % FBS. (c) U251MG cells were treated with biotin-conjugated L4–3 macrocyclic peptide at concentrations of 1 μM and 3 μM for 30 min. The binding of biotin-conjugated L4–3 to CD44 was evaluated after an overnight incubation with 30 μl of streptavidin-conjugated magnetic beads; incubation without beads served as a control (designated as total cell lysate, TCL). Immunoblotting was then performed using CD44 antibodies (Table S1). (d) The proliferation of U251MG cells growing in 3 % FBS, in the absence or presence of macrocyclic peptides (1 μM) for six days, was analyzed. (e) In confluent and quiescent cultures of U251MG, wounds were made (with technical triplicates per well). Then, cultures were incubated overnight in the absence or presence of 50 μg/ml hyaluronan (1000 kDa) or 10 % FBS, with or without macrocyclic peptides (1 μM) and 4-MU (1 mM). The bars represent the fold change in wound closure compared to the quiescent cultures. Graph bars are shown as mean ± SEM based on three independent experiments. *P*-values were calculated using Student's paired *t*-test, with * $p < 0.05$ considered statistically significant compared to the control samples.

expressed by U251MG gliomas and block its hyaluronan binding ability. In contrast, the macrocyclic peptide D4–1, which exhibits a lower affinity for CD44 than L4–3 and D4–3 (Table 1), did not significantly affect their cellular adhesion to immobilized hyaluronan (Fig. 2a). L4–3 and D4–3 also significantly inhibited the adhesion of A549 and Hs578T cells to hyaluronan-coated plates, but had no effect on the adhesion of A549 cells onto collagen coated dishes; also in these cell lines, D4–1 did not affected the adhesion (Fig. S5a, S5c). In addition, the macrocyclic peptides were non-toxic for the cells at the tested concentration of 1 μM. (Fig. 2b and Figs. S5 b,d). A direct interaction between CD44 and biotin-conjugated L4–3 macrocyclic peptide (L4–3-biotin) was demonstrated by a pull-down assay, further confirming the direct interaction between CD44 and L4–3 (Fig. 2c). Of note, the peptides did not affect U251MG cell proliferation (Fig. 2d).

Given that gliomas rarely metastasize, but instead invade surrounding brain structures, and considering that one of the abundant components of the ECM in gliomas is hyaluronan [11,26,40], we investigated the impact of exogenously added hyaluronan on the motility of U251MG glioma cells (Fig. 2e). In a scratch wound healing assay, cultures stimulated with 10 % FBS showed an approximately two-fold increase in motility, whereas cultures stimulated with hyaluronan did not exhibit any significant changes. The addition of L4–3, D4–1, and D4–3 did not affect the motility induced by 10 % FBS. The inhibition of endogenously synthesized hyaluronan in glioma cells, using 4-MU, significantly reduced both their basal motility and the motility stimulated by 10 % FBS. Similarly, 4-MU reduced the cell motility induced by 10 % FBS in A549 lung cancer cells and Hs578T breast cancer cells (Fig. S6 a,b). These findings are consistent with results from our laboratory and others [41], suggesting that the effects of exogenously added hyaluronan are not equivalent to those of endogenously synthesized hyaluronan.

3.3. L4-3 affects PMA-induced CD44 cleavage and PMA-suppressed EGFR phosphorylation, as well as EGFR-mediated AKT activation

CD44, like certain other membrane proteins, can be proteolytically cleaved, liberating the intracellular domain which is important for CD44-mediated tumor cell migration [11,17,40]. PMA stimulation of U251MG cells rapidly induced cleavage of CD44, as depicted by increased CD44 TM-ICD and CD44 ICD products (Fig. 3a). This finding suggests that the cleavage of the standard form of CD44 may influence cell attachment and migration of U251MG cells in a hyaluronan matrix [42]. The macrocyclic peptide L4–3 significantly inhibited the PMA-mediated cleavage of the extracellular domain of CD44, possibly contributing to the reduced glioma cell migration on a hyaluronan matrix.

Given the significance of EGFR in the progression of glioblastoma multiforme [43], along with its role in PMA-mediated tumor promotion and its constitutive interaction with CD44 [44,45], we examined how L4–3 affects the activation status of EGFR (Fig. 3b) and its downstream signaling following stimulation with PMA or EGF (Fig. 4). An approximately 70 % reduction of the phosphorylation of Tyr1068 in EGFR was observed after treatment with PMA, consistent with previous reports [46,47]. Notably, L4–3 further enhanced the PMA-induced negative regulation of EGFR autophosphorylation (Fig. 3b). Moreover, PMA significantly increased the amount of EGFR protein (Fig. 3b). This finding is consistent with earlier findings showing that PMA activation of PKC effectively inhibits downregulation of EGFR, typically induced by the ligand EGF [48,49].

In parallel, PMA stimulation led to increased activation of AKT, ERK1/2, and ERM (ezrin, radixin, and moesin) signaling pathways (Fig. 4a, b and c), *i.e.* signaling pathways important for cell survival, proliferation, adhesion, and membrane ruffling [15,38,42,50]. Stimulation of glioma cells with EGF significantly activated the downstream signaling pathways of AKT and ERK1/2 (Fig. 4d, e), but did not activate the ERM pathway (Fig. 4f). Interestingly, the macrocyclic peptide L4–3 significantly reduced the EGF-induced activation of AKT, but did not have any effect on the ERK1/2 pathway.

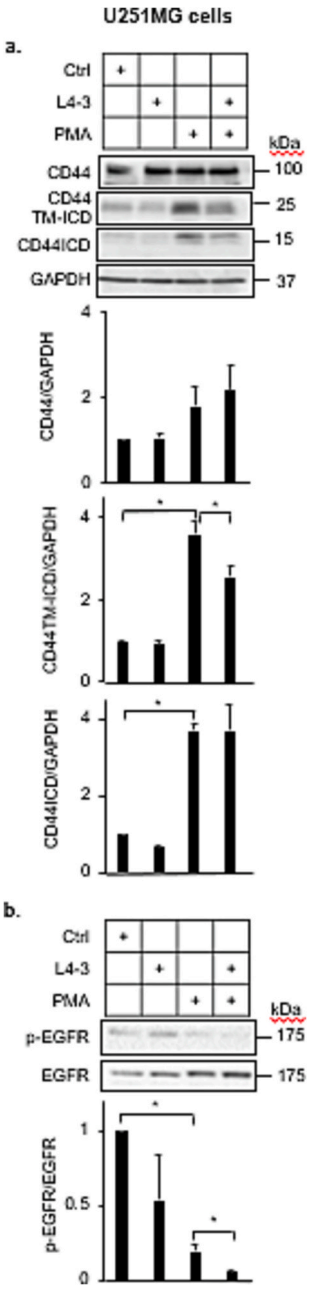

Fig. 3. PMA-mediated cleavage of CD44 and dephosphorylation of *EGFR* are influenced by L4–3. (a,b) U251MG glioma cells grown in starvation medium were pre-treated for 30 min with L4–3 (1 μM), before PMA (80 nM) was added for another 30 min, followed by cell lysis. The cleavage of CD44 induced by PMA generated CD44 TM-ICD and CD44 ICD (a), and the activation status of EGFR by phosphorylation at Tyr1068 (see Table S1) (b), was determined by immunoblotting, as described in Materials and Methods. All graph bars are shown as average ± SEM based on at least three independent experiments. Asterisks illustrate alterations between the samples relative to their respective controls: $*p < 0.05$.

3.4. Fragmented hyaluronan induces cleavage of CD44, but with slower kinetics than PMA

The progression of several cancers is enhanced by chronic inflammation. The generation of inflammatory fragmented hyaluronan in the

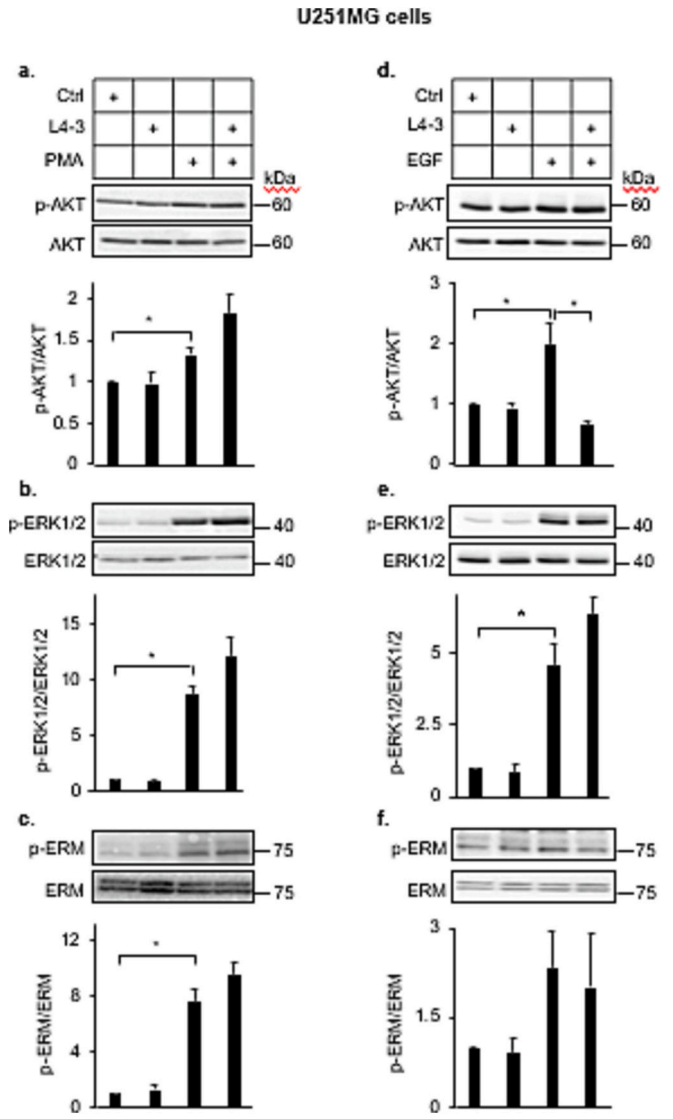

Fig. 4. Downstream signaling pathways activated by PMA and EGF are differently influenced by L4–3. (a-f) U251MG cells were treated with L4–3 (1 μM) for 30 min before 80 nM PMA or 25 ng/ml EGF was added for another 30 min. Then cells were lysed and the activation status of AKT (a, d), ERK (b, e), and ERM (c, f) were visualized by immunoblotting of total cell lysates. All graph bars are shown as average ± SEM based on three independent experiments. Asterisks illustrate alterations between the samples relative to their respective controls: $^{*}p < 0.05$.

surrounding stroma regulate host-tumor communication [51]. Our recent studies demonstrated the pro-tumorigenic properties of the CD44-hyaluronan axis in glioblastomas due to their correlation to growth and stemness, as well as involvement in PDGF signaling [38]. To investigate how fragmented hyaluronan affects CD44 cleavage, glioma cultures were stimulated with hyaluronan of a molecular mass ≤ 200 kDa (HA ≤ 200 kDa) for different time periods (Fig. 5). CD44 ICD products were detected after one hour in a low-molecular-mass hyaluronan-rich environment, which is slower than PMA-induced CD44 cleavage, observed within 30 min (Fig. 5). This observation suggests that the shedding of cell surface CD44 in glioblastomas, and thus the regulation of tumor cell motility on a hyaluronan substrate, is not primarily controlled by hyaluronan-CD44 interactions, but rather influenced by other malignant activities.

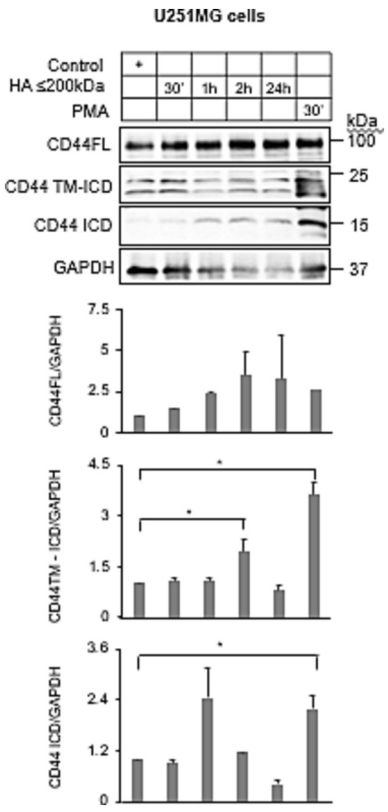

Fig. 5. Hyaluronan of a molecular mass of 200 kDa or less promotes CD44 cleavage, but at a slower rate than PMA. U251MG cells were treated with 50 μg/ml hyaluronan (≤200 kDa) for 30 min, 1, 2, and 24 h, or with 80 nM PMA for 30 min in starvation medium (0.1 % FBS-RPMI-1640), followed by cell lysis. The cleavage of CD44 induced by hyaluronan and PMA, generating CD44 TM-ICD and CD44 ICD, was analyzed by immunoblotting. Graph bars are shown as the mean ± SEM based on three independent experiments. Asterisks represent significant differences between the samples relative to their respective controls: $^{*}p < 0.05$.

3.5. D4-3 reduces fibroblast adherence to immobilized hyaluronan

Given that CD44 is expressed at high levels on fibroblasts, AG1523 human foreskin fibroblasts were used to investigate the CD44-mediated ability to adhere to hyaluronan-coated surfaces in the absence or presence of macrocyclic peptides [52]. In line with the findings from the cancer cells studied, D4–3 significantly decreased the adhesion of fibroblasts to the hyaluronan-coated plates, as did L4–3, but less efficiently than in glioma cells (Fig. 6a). High molecular weight hyaluronan (approximately 1000 kDa; the predominant molecular size of hyaluronan under physiological conditions) did not affect the migration of AG1523 fibroblasts (Fig. 6b), which may be due to the fact that fibroblasts produce endogenous hyaluronan.

Next, we investigated how hyaluronan stimulation affects downstream signaling in the absence or presence of D4–3-engaged CD44. As illustrated in Fig. 7, PDGF-BB, a potent stimulator of fibroblast hyaluronan synthesis through the induction of HAS2 [41], efficiently activated the AKT (pSer473) and ERK1/2 (pThr202/Tyr204) signaling pathways, which support cell survival and proliferation (Fig. 7a and b). Stimulation with hyaluronan did not affect the activation of these signaling pathways, whether or not the macrocyclic peptide D4–3 was present. However, when fibroblast cultures were treated with high molecular weight hyaluronan (approximately 1000 kDa) for 40 min, there was a suppression of the endogenous activation of FAK and ERM; the suppression was further intensified in the presence of D4–3 (see Fig. 7c and d). Thus, D4–3 enhances signaling mediated by hyaluronan and CD44 in

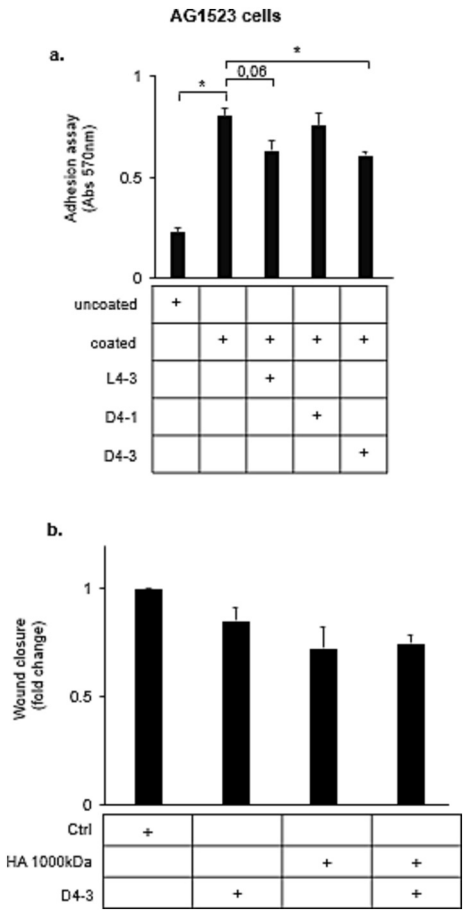

Fig. 6. D4–3 suppresses adhesion of AG1523 fibroblasts to hyaluronan.
(a) Fibroblasts treated with 1 μM of the L4–3, D4–1 or D4–3, or no peptide, were subjected to an adhesion assay in hyaluronan-coated plates. Uncoated wells were used as controls. (b) Wound healing assay of confluent AG1523 cells treated with the macrocyclic peptide D4–3 (1 μM) and 20 μg/ml hyaluronan (1000 kDa) for 12 h. All graph bars are shown as average ± SEM based on three independent experiments. Asterisks illustrate alterations between the samples relative to their respective controls: $*p < 0.05$.

fibroblasts, which is associated with cell adhesion and migration.

4. Discussion

This study highlights the relevance of physical and functional links between CD44 and EGFR in hyaluronan-dependent and -independent manners in glioblastoma progression. Initially, it was assumed that the role of CD44 is to mediate cell adhesion to the extracellular matrix, however, a large body of studies has shown that CD44 also acts as a signaling receptor in co-operation with tyrosine kinase receptors [14]. We demonstrate that the macrocyclic peptides L4–3 and D4–3 interact with the hyaluronan binding region in the CD44 ectodomain, thereby preventing the formation of CD44-hyaluronan complexes and inhibiting the adhesion of CD44-expressing cells onto immobilized hyaluronan (Figs. 2a, S5a,c and 6a). In our previous studies [38], we demonstrated that genetically depleting CD44 from U251MG cells resulted in a significant impairment of their ability to synthesize and bind hyaluronan, as well as a reduction in proliferation and stemness. Furthermore, glioma cells lacking CD44 showed strong adhesion to dishes coated with collagen type I and fibronectin. Notably, the ablation of CD44 or the inhibition of CD44 cleavage severely disrupted autocrine signaling and the expression of members of the PDGF family. High-grade gliomas show elevated levels of RHAMM [53], which interacts with the transmembrane receptors for EGF and PDGF, along with CD44. Gene amplifications of *EGFR* and/or *PDGFR* are associated with changes in ECM molecules, for example aggrecan which binds hyaluronan [23]. However, the relationship between these molecular changes and the amounts of hyaluronan in the ECM remains unclear.

The EGFR signaling is regulated by both trans-regulatory homologous and heterologous mechanisms [54] that influence the duration of downstream signaling, impacting tumor promotion and the activation of hyaluronan-engaged CD44 during glioma progression [24,44,55]. Phosphorylation of the EGF receptor by protein PKC was shown to decrease the affinity of EGF binding to EGFR and to reduce the receptor kinase activity. In membrane preparations, phosphorylation of EGFR by protein kinase C resulted in conversion of high affinity EGF binding sites to low affinity sites [56]. However, the underlying molecular mechanisms are not well understood [57] and contradictory observations have been made [23,58].

Stimulation with PMA led to significant sequential cleavage of CD44 and a decrease in EGFR autophosphorylation at Tyr1068, along with a concurrent increase in EGFR expression (Fig. 3b). These findings align with previous research showing that PMA activates PKC, which phosphorylates EGFR at Thr654 [48]. This process effectively prevents the internalization, downregulation and degradation of EGFR typically triggered by the ligand EGF, emphasizing PMA's vital role in regulation of EGFR signaling. However, PMA stimulation also results in the downregulation of EGFR Tyr1068 through ERK1/2-mediated phosphorylation at Thr669 [47]. The phosphorylation of Tyr1068 in EGFR activates downstream signaling pathways, including the RAS-RAF-MEK-ERK1/2 and PI3K-AKT pathways, which contribute to tumor progression. Importantly, the macrocyclic peptide L4–3 significantly suppressed CD44 cleavage (Fig. 3a) and inhibited EGF-mediated AKT phosphorylation (Fig. 4d) without affecting ERK1/2 and ERM phosphorylation, suggesting that L4–3 may regulate EGFR signaling. Full-length CD44 consistently interacts with both the full-length EGFR and its truncated variant, EGFRvIII. Additionally, CD44, when engaged with hyaluronan, influences gene expression through an EGFR-dependent pathway [44]. Therefore, our findings support the notion that L4–3 prevents CD44 cleavage and facilitates EGFR-CD44 interactions in U251MG cells.

Moreover, PMA and growth factors, like EGF and PDGF-BB, strongly stimulate hyaluronan synthesis, mainly by inducing HAS2 expression. HAS2 is crucial for EGF-mediated activation of the FAK-PI3K-AKT signaling pathway in aggressive breast cancer cells [59,60]. This might help explain why L4–3 disrupts the natural interactions between the EGFR and hyaluronan-activated CD44, which leads to the activation of AKT, while not affecting EGFR-mediated ERK1/2 activation. While no changes in ERM activity were observed, a redistribution of CD44 and ERM proteins to newly generated areas of membrane ruffling may have occurred, which could enhance glioma cell migration (Fig. 4f). This observation suggests that hyaluronan-activated CD44 is important for EGFR-mediated AKT activation.

Our previous studies have demonstrated that PDGF-BB is a powerful stimulator of the proliferation and migration of human breast-derived fibroblasts [59]. The ERK1/2-MAPK and PI3K-AKT signaling pathways play crucial roles in PDGF-BB-mediated hyaluronan synthesis in these cultures. Additionally, preventing the binding of hyaluronan to CD44 inhibits fibroblast growth. Furthermore, the activation of CD44 by hyaluronan suppresses fibroblast migration induced by the PDGF β-receptor [61]. Considering that FAK plays a significant role in promoting PDGF- and EGF-stimulated cell migration [62], the D4–3-mediated suppression of FAK and ERM phosphorylation may have physiological relevance in pathophyisiological conditions, such as wound healing.

Targeted therapies of glioblastoma have not yet shown any clinical benefit. Although the understanding of cellular signaling has advanced, the tumor heterogeneity, mutations and compensatory signaling pathways, require an integrated approach to elucidate the underlying molecular mechanisms.

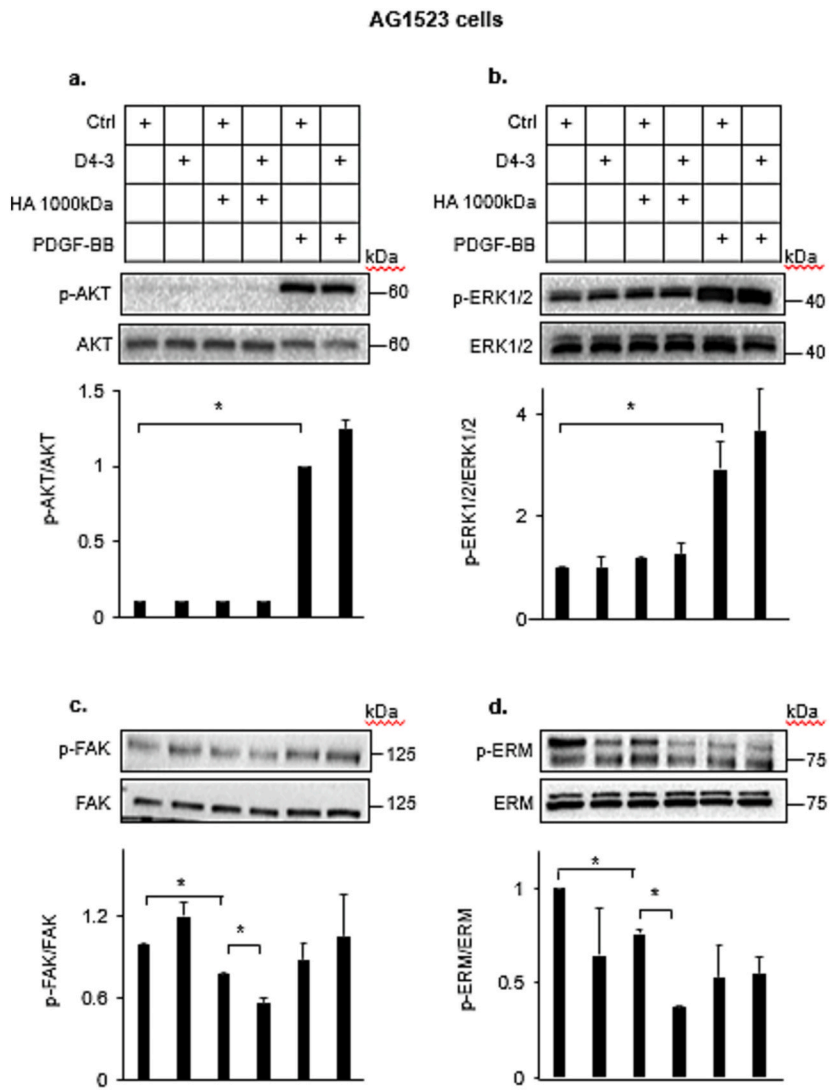

Fig. 7. Effect of D4–3 on the activation of signaling molecules in fibroblast AG1523 cells. (a-d) Total cell lysates of AG1523 cells after treatment with 1 μM D4–3 in 0.1 % FBS/DMEM for 30 min prior to stimulation with 20 μg/ml hyaluronan (1000 kDa) for an additional 40 min, or stimulation with 20 ng/ml PDGF-BB for 10 min, were subjected to SDS-PAGE. The phosphorylation of AKT (a), ERK1/2 (b), FAK (c) and ERM (d) was then determined by immunoblotting. Phosphorylated protein bands were quantified by the software ImageJ and normalized to the total amount of the respective proteins, and expressed as fold difference. Graph bars are shown as the average ± SEM based on three independent experiments. Asterisks illustrate significant difference between the different conditions, compared to the respective control samples: * $p < 0.05$.

CRediT authorship contribution statement

Athanasios Chatzopoulos: Writing – review & editing, Writing – original draft, Visualization, Validation, Software, Methodology, Formal analysis, Data curation. **Constantinos Kolliopoulos:** Writing – review & editing, Visualization, Validation, Software, Methodology, Data curation. **Yizhen Yin:** Writing – review & editing, Visualization, Validation, Software, Methodology, Data curation. **Theodoros Karalis:** Writing – review & editing, Visualization, Validation, Software, Methodology. **Aya Komine:** Writing – review & editing, Visualization, Validation, Software, Methodology. **Sophie T. PhuongDung Tran:** Writing – review & editing, Visualization, Validation, Software, Methodology. **Jongchan Hwang:** Writing – review & editing, Visualization, Validation, Software, Methodology. **Nohara Goto:** Writing – review & editing, Visualization, Validation, Software, Methodology. **Hiroaki Suga:** Writing – review & editing, Conceptualization. **Peter ten Dijke:** Writing – review & editing, Conceptualization. **Christopher John Hipolito:** Writing – review & editing, Validation, Supervision, Formal analysis, Conceptualization. **Spyridon S. Skandalis:** Writing – review & editing, Validation, Supervision, Formal analysis, Conceptualization. **Paraskevi Heldin:** Writing – review & editing, Writing – original draft, Visualization, Validation, Supervision, Software, Resources, Project administration, Methodology, Investigation, Funding acquisition, Formal analysis, Data curation, Conceptualization.

Declaration of competing interest

The authors declare no conflicts of interest.

Acknowledgments

The authors would like to thank C—H Heldin for support and constructive criticism of this work. This work was supported by grants from the Swedish Cancer Society (180657 and 222363).

Appendix A. Supplementary data

Supplementary data to this article can be found online at https://doi.

org/10.1016/j.cellsig.2025.112178.

Data availability

All study data are included in the article.

References

[1] N. Kobayashi, S. Miyoshi, T. Mikami, H. Koyama, M. Kitazawa, M. Takeoka, K. Sano, J. Amano, Z. Isogai, S. Niida, K. Oguri, M. Okayama, J.A. McDonald, K. Kimata, S. Taniguchi, N. Itano, Hyaluronan deficiency in tumor stroma impairs macrophage trafficking and tumor neovascularization, Cancer Res. 70 (2010) 7073–7083.

[2] C. Kolliopoulos, C.Y. Lin, C.H. Heldin, A. Moustakas, P. Heldin, Has2 natural antisense RNA and Hmga2 promote Has2 expression during TGFbeta-induced EMT in breast cancer, Matrix Biol. 80 (2019) 29–45.

[3] P. Heldin, C.Y. Lin, C. Kolliopoulos, Y.H. Chen, S.S. Skandalis, Regulation of hyaluronan biosynthesis and clinical impact of excessive hyaluronan production, Matrix Biol. 78-79 (2019) 100–117.

[4] P. Heldin, T. Asplund, D. Ytterberg, S. Thelin, T.C. Laurent, Characterization of the molecular mechanism involved in the activation of hyaluronan synthetase by platelet-derived growth factor in human mesothelial cells, Biochem. J. 283 (1992) 165–170.

[5] K.L. Mooney, W. Choy, S. Sidhu, P. Pelargos, T.T. Bui, B. Voth, N. Barnette, I. Yang, The role of CD44 in glioblastoma multiforme, J. Clin. Neurosci. 34 (2016) 1–5.

[6] P. Heldin, C. Kolliopoulos, C.Y. Lin, C.H. Heldin, Involvement of hyaluronan and CD44 in cancer and viral infections, Cell. Signal. 65 (2020) 109427.

[7] R.L. Klank, S.A. Decker Grunke, B.L. Bangasser, C.L. Forster, M.A. Price, T.J. Odde, K.S. SantaCruz, S.S. Rosenfeld, P. Canoll, E.A. Turley, J.B. McCarthy, J.R. Ohlfest, D.J. Odde, Biphasic dependence of glioma survival and cell migration on CD44 expression level, Cell Rep. 19 (2017) 668.

[8] D. Naor, R.V. Sionov, D. Ish-Shalom, CD44: structure, function, and association with the malignant process, Adv. Cancer Res. 71 (1997) 241–319.

[9] H. Ponta, D. Wainwright, P. Herrlich, The CD44 protein family, Int. J. Biochem. Cell Biol. 30 (1998) 299–305.

[10] H. Ponta, L. Sherman, P.A. Herrlich, CD44: from adhesion molecules to signalling regulators, Nat. Rev. Mol. Cell Biol. 4 (2003) 33–45.

[11] I. Okamoto, Y. Kawano, H. Tsuiki, J. Sasaki, M. Nakao, M. Matsumoto, M. Suga, M. Ando, M. Nakajima, H. Saya, CD44 cleavage induced by a membrane-associated metalloprotease plays a critical role in tumor cell migration, Oncogene 18 (1999) 1435–1446.

[12] D. Murakami, I. Okamoto, O. Nagano, Y. Kawano, T. Tomita, T. Iwatsubo, B. De Strooper, E. Yumoto, H. Saya, Presenilin-dependent gamma-secretase activity mediates the intramembranous cleavage of CD44, Oncogene 22 (2003) 1511–1516.

[13] I. Okamoto, Y. Kawano, M. Matsumoto, M. Suga, K. Kaibuchi, M. Ando, H. Saya, Regulated CD44 cleavage under the control of protein kinase C, calcium influx, and the rho family of small G proteins, J. Biol. Chem. 274 (1999) 25525–25534.

[14] V. Orian-Rousseau, H. Ponta, Adhesion proteins meet receptors: a common theme? Adv. Cancer Res. 101 (2008) 63–92.

[15] C. Chen, S.J. Zhao, A. Karnad, J.W. Freeman, The biology and role of CD44 in cancer progression: therapeutic implications, J. Hematol. Oncol. 11 (2018).

[16] D. Naor, S.B. Wallach-Dayan, M.A. Zahalka, R.V. Sionov, Involvement of CD44, a molecule with a thousand faces, in cancer dissemination, Semin. Cancer Biol. 18 (2008) 260–267.

[17] I. Okamoto, H. Tsuiki, L.C. Kenyon, A.K. Godwin, D.R. Emlet, M. Holgado-Madruga, I.S. Lanham, C.J. Joynes, K.T. Vo, A. Guha, M. Matsumoto, Y. Ushio, H. Saya, A.J. Wong, Proteolytic cleavage of the CD44 adhesion molecule in multiple human tumors, Am. J. Pathol. 160 (2002) 441–447.

[18] S.S. Skandalis, CD44 intracellular domain: A long tale of a short tail, Cancers 15 (2023).

[19] E. Pure, R.K. Assoian, Rheostatic signaling by CD44 and hyaluronan, Cell. Signal. 21 (2009) 651–655.

[20] B. Huang, X. Li, Y. Li, J. Zhang, Z. Zong, H. Zhang, Current immunotherapies for glioblastoma multiforme, Front. Immunol. 11 (2020) 603911.

[21] M.S. Uddin, A.A. Mamun, B.S. Alghamdi, D. Tewari, P. Jeandet, M.S. Sarwar, G. M. Ashraf, Epigenetics of glioblastoma multiforme: from molecular mechanisms to therapeutic approaches, Semin. Cancer Biol. 83 (2022) 100–120.

[22] E.C. Holland, Glioblastoma multiforme: the terminator, Proc. Natl. Acad. Sci. USA 97 (2000) 6242–6244.

[23] M.A. Pibuel, D. Poodts, M. Diaz, S.E. Hajos, S.L. Lompardia, The scrambled story between hyaluronan and glioblastoma, J. Biol. Chem. 296 (2021) 100549.

[24] A. Oprita, S.C. Baloi, G.A. Staicu, O. Alexandru, D.E. Tache, S. Danoiu, E.S. Micu, A.S. Sevastre, Updated insights on EGFR signaling pathways in glioma, Int. J. Mol. Sci. (2021) 22.

[25] J. Baselga, Targeting tyrosine kinases in cancer: the second wave, Science 312 (2006) 1175–1178.

[26] A. do Carmo, J. Balca-Silva, D. Matias, M.C. Lopes, PKC signaling in glioblastoma, Cancer Biol. Ther. 14 (2013) 287–294.

[27] T. Passioura, The road ahead for the development of macrocyclic peptide ligands, Biochemistry 59 (2020) 139–145.

[28] T. Morioka, N.D. Loik, C.J. Hipolito, Y. Goto, H. Suga, Selection-based discovery of macrocyclic peptides for the next generation therapeutics, Curr. Opin. Chem. Biol. 26 (2015) 34–41.

[29] K. Ito, K. Sakai, Y. Suzuki, N. Ozawa, T. Hatta, T. Natsume, K. Matsumoto, H. Suga, Artificial human met agonists based on macrocycle scaffolds, Nat. Commun. 6 (2015).

[30] K. Ito, T. Passioura, H. Suga, Technologies for the synthesis of mRNA-encoding libraries and discovery of bioactive natural product-inspired non-traditional macrocyclic peptides, Molecules 18 (2013) 3502–3528.

[31] T. Wahlstrom, E. Linder, E. Saksela, B. Westermark, Tumor-specific membrane antigens in established cell lines from gliomas, Cancer 34 (1974) 274–279.

[32] Y. Hayashi, J. Morimoto, H. Suga, Selection of anti-Akt2 thioether-macrocyclic peptides leading to isoform-selective inhibitors, ACS Chem. Biol. 7 (2012) 607–613.

[33] H. Niwa, S. Masui, I. Chambers, A.G. Smith, J. Miyazaki, Phenotypic complementation establishes requirements for specific POU domain and generic transactivation function of Oct-3/4 in embryonic stem cells, Mol. Cell. Biol. 22 (2002) 1526–1536.

[34] J. Fujikura, E. Yamato, S. Yonemura, K. Hosoda, S. Masui, K. Nakao, J. Miyazaki, H. Niwa, Differentiation of embryonic stem cells is induced by GATA factors, Genes Dev. 16 (2002) 784–789.

[35] S. Yamada, S. Itai, T. Nakamura, M. Yanaka, M.K. Kaneko, Y. Kato, Detection of high CD44 expression in oral cancers using the novel monoclonal antibody, CMab-5, Biochem. Biophys. Rep. 14 (2018) 64–68.

[36] M. Feoktistova, P. Geserick, M. Leverkus, Crystal violet assay for determining viability of cultured cells, Cold Spring Harb Protoc 2016 (2016) pdb prot087379.

[37] C. Kolliopoulos, A. Chatzopoulos, S.S. Skandalis, C.H. Heldin, P. Heldin, TRAF4/6 is needed for CD44 cleavage and migration via RAC1 activation, Cancers (Basel) 13 (2021).

[38] C. Kolliopoulos, M.M. Ali, C. Castillejo-Lopez, C.H. Heldin, P. Heldin, CD44 depletion in glioblastoma cells suppresses growth and stemness and induces senescence, Cancers 14 (2022).

[39] T. Karalis, A.K. Shiau, T.C. Gahman, S.S. Skandalis, C.H. Heldin, P. Heldin, Identification of a small molecule inhibitor of hyaluronan synthesis, DDIT, targeting breast cancer cells, Cancers (Basel) (2022) 14.

[40] Z. Werb, ECM and cell surface proteolysis: regulating cellular ecology, Cell 91 (1997) 439–442.

[41] Y. Li, L. Li, T.J. Brown, P. Heldin, Silencing of hyaluronan synthase 2 suppresses the malignant phenotype of invasive breast cancer cells, Int. J. Cancer 120 (2007) 2557–2567.

[42] O. Nagano, H. Saya, Mechanism and biological significance of CD44 cleavage, Cancer Sci. 95 (2004) 930–935.

[43] A.J. Ekstrand, C.D. James, W.K. Cavenee, B. Seliger, R.F. Pettersson, V.P. Collins, Genes for epidermal growth factor receptor, transforming growth factor alpha, and epidermal growth factor and their expression in human gliomas in vivo, Cancer Res. 51 (1991) 2164–2172.

[44] D. Tsatas, V. Kanagasundaram, A. Kaye, U. Novak, EGF receptor modifies cellular responses to hyaluronan in glioblastoma cell lines, J. Clin. Neurosci. 9 (2002) 282–288.

[45] T. Gulliford, X. Ouyang, R.J. Epstein, Intensification of growth factor receptor signalling by phorbol treatment of ligand-primed cells implies a dimer-stabilizing effect of protein kinase C-dependent juxtamembrane domain phosphorylation, Cell. Signal. 11 (1999) 245–252.

[46] G. Sette, V. Salvati, M. Mottolese, P. Visca, E. Gallo, K. Fecchi, E. Pilozzi, E. Duranti, E. Policicchio, M. Tartaglia, M. Milella, R. De Maria, A. Eramo, Tyr1068-phosphorylated epidermal growth factor receptor (EGFR) predicts cancer stem cell targeting by erlotinib in preclinical models of wild-type EGFR lung cancer, Cell Death Dis. 6 (2015).

[47] R.D. Haryuni, T. Tanaka, Y. Zhou, S. Yokoyama, H. Sakurai, ERK-mediated negative feedback regulation of oncogenic EGFRvIII in glioblastoma cells, Oncol. Lett. 20 (2020) 2477–2482.

[48] J. Bao, I. Alroy, H. Waterman, E.D. Schejter, C. Brodie, J. Gruenberg, Y. Yarden, Threonine phosphorylation diverts internalized epidermal growth factor receptors from a degradative pathway to the recycling endosome, J. Biol. Chem. 275 (2000) 26178–26186.

[49] T. Hunter, N. Ling, J.A. Cooper, Protein kinase C phosphorylation of the EGF receptor at a threonine residue close to the cytoplasmic face of the plasma membrane, Nature 311 (1984) 480–483.

[50] T. Ando, J. Yamasaki, H. Saya, O. Nagano, CD44: a key regulator of iron metabolism, redox balance, and therapeutic resistance in cancer stem cells, Stem Cells 43 (2025).

[51] D. Nikitovic, M. Tzardi, A. Berdiaki, A. Tsatsakis, G.N. Tzanakakis, Cancer microenvironment and inflammation: role of hyaluronan, Front. Immunol. 6 (2015) 169.

[52] R.J.S. Sneath, D.C. Mangham, The normal structure and function of CD44 and its role in neoplasia, J. Clin. Pathol. 51 (1998) 191–200.

[53] Y. Akiyama, S. Jung, B. Salhia, S.P. Lee, S. Hubbard, M. Taylor, T. Mainprize, K. Akaishi, W. van Furth, J.T. Rutka, Hyaluronate receptors mediating glioma cell migration and proliferation, J. Neuro-Oncol. 53 (2001) 115–127.

[54] Y. Yarden, A. Ullrich, Growth factor receptor tyrosine kinases, Annu. Rev. Biochem. 57 (1988) 443–478.

[55] J.X. Li, C.L. Ma, Y. Huang, H. Luo, C.S. Huang, Differential requirement of EGF receptor and its tyrosine kinase for AP-1 transactivation induced by EGF and TPA, Oncogene 22 (2003) 211–219.

[56] J. Downward, M.D. Waterfield, P.J. Parker, Autophosphorylation and protein kinase-C phosphorylation of the epidermal growth-factor receptor - effect on tyrosine kinase-activity and ligand-binding affinity, J. Biol. Chem. 260 (1985) 4538–4546.

[57] J.B. Park, H.J. Kwak, S.H. Lee, Role of hyaluronan in glioma invasion, Cell Adhes. Migr. 2 (2008) 202–207.
[58] S. Amos, P.M. Martin, G.A. Polar, S.J. Parsons, I.M. Hussaini, Phorbol 12-myristate 13-acetate induces epidermal growth factor receptor transactivation via protein kinase Cdelta/c-Src pathways in glioblastoma cells, J. Biol. Chem. 280 (2005) 7729–7738.
[59] L. Li, T. Asteriou, B. Bernert, C.H. Heldin, P. Heldin, Growth factor regulation of hyaluronan synthesis and degradation in human dermal fibroblasts: importance of hyaluronan for the mitogenic response of PDGF-BB, Biochem. J. 404 (2007) 327–336.
[60] B. Bernert, H. Porsch, P. Heldin, Hyaluronan synthase 2 (HAS2) promotes breast cancer cell invasion by suppression of tissue metalloproteinase inhibitor 1 (TIMP-1), J. Biol. Chem. 286 (2011) 42349–42359.
[61] L. Li, C.H. Heldin, P. Heldin, Inhibition of platelet-derived growth factor-BB-induced receptor activation and fibroblast migration by hyaluronan activation of CD44, J. Biol. Chem. 281 (2006) 26512–26519.
[62] D.J. Sieg, C.R. Hauck, D. Ilic, C.K. Klingbeil, E. Schaefer, C.H. Damsky, D. D. Schlaepfer, FAK integrates growth-factor and integrin signals to promote cell migration, Nat. Cell Biol. 2 (2000) 249–256.